ISSN 0016-7932, Geomagnetism and Aeronomy, 2006, Vol. 46, No. 4, pp. 430–437. © Pleiades Publishing, Inc., 2006.
Original Russian Text © A.V. Belov, V.N. Obridko, B.D. Shelting, 2006, published in Geomagnetizm i Aeronomiya, 2006, Vol. 46, No. 4, pp. 456–464.

Correlation between the Near-Earth Solar Wind Parameters and the Source Surface Magnetic Field

A. V. Belov, V. N. Obridko, and B. D. Shelting

Institute of Terrestrial Magnetism, Ionosphere, and Radiowave Propagation, Russian Academy of Sciences, Troitsk, Moscow oblast, 142190 Russia

Received February 16, 2005

Abstract—The solar magnetic field B_s at the Earth's projection onto the solar-wind source surface has been calculated for each day over a long time interval (1976–2004). These data have been compared with the daily mean solar wind (SW) velocities and various components of the interplanetary magnetic field (IMF) near the Earth. The statistical analysis has revealed a rather close relationship between the solar-wind parameters near the Sun and near the Earth in the periods without significant sporadic solar and interplanetary disturbances. Empirical numerical models have been proposed for calculating the solar-wind velocity, IMF intensity, and IMF longitudinal and B_z components from the solar magnetic data. In all these models, the B_s value plays the main role. It is shown that, under quiet or weakly disturbed conditions, the variations in the geomagnetic activity index *Ap* can be forecasted for 3–5 days ahead on the basis of solar magnetic observations. Such a forecast proves to be more reliable than the forecasts based on the traditional methods.

PACS numbers: 96.50.Ci

DOI: 10.1134/S0016793206040049

1. INTRODUCTION

Solar plasma reaches the Earth after having crossed the solar-wind source surface a few days earlier. Therefore, it seems obvious that the knowledge of the plasma characteristics on the source surface would enable us to predict the behavior of the solar wind (SW) near the Earth. Moreover, since the geomagnetic disturbances are controlled by the local parameters of the solar wind [Akasofu, 1981], we could also forecast geomagnetic activity. It is most promising to predict various components of the interplanetary magnetic field (IMF) and solar wind velocity. The photospheric magnetic field is regularly measured; the models were developed [Hoeksema and Scherrer, 1986] for calculating the source-surface field on the basis of photospheric observations. Rather long ago, Wang and Sheeley [1990, 1991, 1992] proposed a method for determining the solar wind velocity from the same magnetic data and proved its efficiency. However, all these data and techniques are still insufficiently used in the space weather problems, and a comprehensive method for forecasting the interplanetary parameters and geomagnetic indices based on solar magnetic observations has not yet been developed. Several basic problems can explain such a situation. Firstly, the solar wind changes significantly on its way from the Sun to the Earth. While the magnetic field on the source surface is assumed to be strictly radial with the transverse component absent, the actual IMF observations reveal a strong variability of its direction. The transverse component (in particular, B_z) does not only exist in the actual field but is comparable with the longitudinal component. It is even alleged sometimes that the magnetic field observed near the Earth is mostly of an interplanetary origin. Secondly, though the models for calculating the solar magnetic field under potential approximation are widely and successfully applied, they are still limited and incomplete. In particular, these models are absolutely inapplicable to all nonstationary situations. Thirdly, the completeness and accuracy of the experimental data are often far from perfect. This concerns both solar observations and solar wind measurements. These are, probably, the reasons why exact quantitative estimates of the coupling between the circumsolar and near-Earth parameters of the solar wind are not available and the practical value of such coupling has not been proved.

In this paper, we statistically analyze the relation between the solar wind velocity and IMF components measured near the Earth and the solar magnetic field calculated for the source surface. The objective of the study is to find out how close this relation is and to quantitatively describe this relation, which can be used in a short-term forecast of the near-Earth solar-wind parameters and geomagnetic activity.

2. DATA AND METHODS

The study is based on using the magnetic field intensity B_s at the Earth's projection onto the solar-wind source surface determined for each day. Besides, we have used the photospheric magnetic field B_p at the conjugate point. The values B_s and B_p were found by the

method developed in [Obridko et al., 2006]. In this work, all commonly used calculation patterns and original databases were analyzed from a single standpoint. It was shown that the applied assumptions and limitations could not impair the general structure and cycle dependence of either the solar or interplanetary data. On the other hand, the measured solar field is underrated as a result of the signal saturation effect in magnetographs. It was shown that the correction must depend on both the heliocentric latitude of observation and the phase of the cycle. A correction method was proposed that ensured a good agreement between the calculated and measured values. The created database made it possible to quantitatively calculate the magnetic fields in the solar wind near the Earth.

The solar magnetic data were compared with the daily mean solar wind velocities and IMF parameters taken from the OMNI database (http://nssdc.gsfc.nasa.gov/omniweb/ow.html). As a result, we had at our disposal the data for more than 28 years (from the end of May 1976 to September 2004). However, far from all these data could be used to establish quantitative relations.

The recent IMF and SW-velocity data in the OMNI catalog (beginning with 1995 and, especially, with 1998) are sufficiently complete. Previously, the situation was much worse and changed from a relatively satisfactory in 1979–1981 to the total lack of the velocity measurements in the late 1982 and early 1983. The preliminary calculations performed by us indicated that it is insufficient to have measurements on a given day. It is desirable that the daily mean SW velocities and IMF parameters were based on sufficiently full measurements. The best results are obtained for the days when the solar wind measurements were carried out around the clock. The period under investigation comprises about 42% of such days.

The solar magnetic data are even less complete. The Stanford ground-based measurements used in our work depend on the weather and contain a lot of gaps, especially, in winter. Since the source-surface field is calculated from the synoptic charts, the values for each day are determined from the measurements obtained during a full solar rotation. We have introduced a simple quality index: the number of days of the Stanford measurements available for the 27-day interval centered on a given day. As in the case of the solar wind, preliminary calculations have shown a significant dependence on the quality (completeness) of data. The more rigorous quality criterion was applied the better were the results. The best result was obtained with the fullest data (27 days of measurements per rotation). The period under discussion comprised only 15% of such days. Moreover, an attempt to ensure completeness of both the solar and interplanetary data (which is very desirable) will leave only one of every 15 days for the analysis.

The approach used by us imposes considerable additional limitations. From the very beginning, it was clear that only relatively slow variations in interplanetary conditions due to the recurrent phenomena and evolution of large-scale solar fields could be forecasted on the basis of the synoptic charts of the solar magnetic field and daily mean data. The sporadic events on the Sun can considerably change the background conditions in the solar wind. It is obvious that this approach is absolutely useless for the days when interplanetary disturbances associated with the coronal mass ejections (CMEs) arrive at the Earth. Such days must be excluded from the analysis, which we tried to do. First of all, we eliminated the days when interplanetary shock waves producing storm sudden commencements (SSCs) were observed near the Earth. The shock wave is often followed by the proper ejection, and the interplanetary conditions are far from quasi-stationary for a few days. Therefore, besides the SSC day, we had to exclude the following three days. Note that this limitation substantially decreases the ejection effect but slightly influence the effects associated with the coronal holes, since the arrival of high-speed solar wind streams from the latter is not usually accompanied by interplanetary shocks. Then, we excluded the days of very strong and severe magnetic storms, when the maximum 3-h *Kp* index was equal to or exceeded 8_. Such magnetic storms are always associated with CME events, and this limitation has even smaller influence the coronal-hole effects than the previous one. This is, probably, the mildest of the used criteria; it rejects only 1% of the data. It should be taken into account that not all CMEs produce interplanetary shocks and/or severe magnetic storms. A significant part of the ejected solar matter reaching the Earth is not preceded by a shock and causes relatively small geomagnetic disturbances. In particular, this concerns the ejections associated with the disappearing solar filaments. Even in these cases, however, the nonstationary nature of the near-Earth phenomena is evident, and the corresponding days must also be excluded from the analysis. For this purpose, we additionally filtered out the days of increased solar wind density N_{SW} and intensity B of the interplanetary magnetic field. In so doing, we kept in all days with the daily mean values $N_{SW} < 10$ particle^{-1} cm^{-3} and $B_{\mathrm{IMF}} < 10$ nT even at the most strict selection. The criteria of the data filtration mentioned above often duplicate one another and, on the whole, only about one third of the days were excluded. Thus, the approach under discussion, in spite of its obvious limitation, is applicable to most situations in the near-Earth space and to about two thirds of the days.

3. RESULTS

Time delay. The solar-wind velocity model to be discussed in the next section was used to study the effect of the time delay. The dispersion between the measured and calculated velocities was minimal for the delay $\tau = 4$ days, was somewhat greater for 5 days, and was much greater for the other delay times. Approximating the dispersion dependence on τ by the fourth

order polynomial, we obtain the optimal delay time $\tau = 4.2 \pm 0.6$ days, which corresponds to the mean solar-wind velocity between the Sun and the Earth equal to 411 ± 58 km/s. This value is close to the mean solar-wind velocity near the Earth in our sample (428 ± 5 km/s). By setting a single delay time of 4 or 5 days for the whole sample, we obtain quite satisfactory results. They will be even better, however, if we use the observed solar wind velocity V_{SW} and assume that $\tau = R_E/V_{SW}$ ($R_E = 1$ AU). The value of τ determined from this expression and rounded to an integer number of days is used in all models discussed below.

Solar-wind velocity model. Wang and Sheeley [1990, 1991] introduced the parameter characterizing the divergence of the field lines. To calculate this parameter, we must, first, determine the magnetic field structure in a spherical layer between the photosphere and the source surface. Then, the field line is traced from the Earth's helioprojection onto the source surface to the photosphere. The magnetic fields at the beginning and the end of this field line are used to calculate the above-mentioned parameter. In our work, we have used the parameter [Obridko et al., 1996] inverse in magnitude to that proposed by Wang and Sheeley [Wang and Sheeley, 1990]. In so doing, we assumed the radius of the source surface to be equal to 2.5 solar radii. It is obvious that $W_s = 1.0$ if the field lines are strictly radial and $W_s < 1.0$ in the other cases

$$W_s = 6.25\left(\frac{B_s}{B_p}\right)^2. \quad (1)$$

First, we checked the agreement between the SW velocity and the Wang–Sheeley parameter W_s for the sampled daily mean values. Taking into account the relation between the solar wind velocity and density, we did not restrict the density N_{SW} in the models for the solar wind velocity V_{SW} but used all other limitations discussed above. The correlation coefficient between W_s and V_{SW} was found to be $\rho = 0.49$ with the rms residual $\sigma = 91.3$ km/s. Such a correlation between the daily mean unsmoothed values is encouraging. However, this is not the best possible one-parameter model. The correlation between $|B_s|$ and V_{SW} proved to be even better with the correlation coefficient equal to 0.53 and the rms residual of 88.7 km/s. As a rule, the stronger the magnetic field at the source surface, the faster the plasma outflow from that region. It is surprising that the modulus of B_s is more closely related to the solar wind velocity than the parameter specially developed to estimate the latter. Of course, it does not matter which parameter gives higher correlation. It is much more important that $|B_s|$ can be combined with W_s in a two-parameter velocity model and that both parameters fortunately complement one another. A small but statistically significant additional improvement of the model can be ensured by introducing the modulus of the photospheric field $|B_p|$ as the third parameter. Choosing the coefficients by the least-square method, we obtain the following velocity model:

$$V_{SW}(t) = (393 \pm 8) + (193 \pm 40)W_s + (3.9 \pm 0.4)|B_s| - (0.019 \pm 0.004)|B_p|, \quad (2)$$

where B_s and B_p are measured in microteslas, and $V_{SW}(t)$, in km/s; hereafter, all solar parameters are determined at instant t–τ.

Figure 1 demonstrates a fairly good agreement ($\rho = 0.64$, $\sigma = 81.2$ km/s) between the calculated and actual velocities for the model under discussion. As seen from the mean values determined for various intervals of the velocity variation, the relation is close to linear.

Because of many gaps in data, it is not so easy to compare the expected and real behavior of V_{SW}. Figure 2 shows the expected velocities calculated according to Eq. (2) for several months of 2004 not only for the days satisfying the data selection criteria but for almost all days when solar magnetic data were available. One can see that such a deliberately roughened model adequately represents the alternation of high- and low-speed solar-wind streams near the Earth.

Model of the IMF longitudinal component. Let us compare the IMF radial component B_{xe} measured near the Earth with B_s recorded τ days earlier (Fig. 3). We will use only the days with full data coverage and the limitations discussed above: no strong magnetic storms, SSC absent on the day under examination and three preceding days, $B_{IMF} < 10$ nT, and $N_{SW} < 10$ particle^{-1} cm^{-3}.

Figure 3 illustrates the coupling between B_s and B_{xe}. For 84% of the days, the sign of B_s coincides with the IMF polarity. At large $|B_s|$ values, the polarities coincide almost completely. On the other hand, the situation is far from ideal. The relation between B_s and B_{xe} is obviously nonlinear, and at small $|B_s|$, the polarities are often mixed. One can readily see that the magnetic field intensity close to zero is much more frequently observed at the source surface than near the Earth. This becomes even more evident if we compare the distributions of B_s and B_{xe} in magnitude (Fig. 4). The discrepancy may be partly due to a lower accuracy of determining the source-surface magnetic field compared to the accuracy of interplanetary measurements, but we also conjecture more serious physical reasons at the background.

The comparison of the distributions shows that weak solar fields do not usually reach the Earth. As was noted earlier [Obridko et al., 2004], the spherical source surface with a strictly radial magnetic field at all points is a mere abstraction. The real magnetic field cannot be radial all over the sphere. It expands below the source surface and, in some regions (e.g., over the coronal holes), does not either remain radial above it. In the pro-

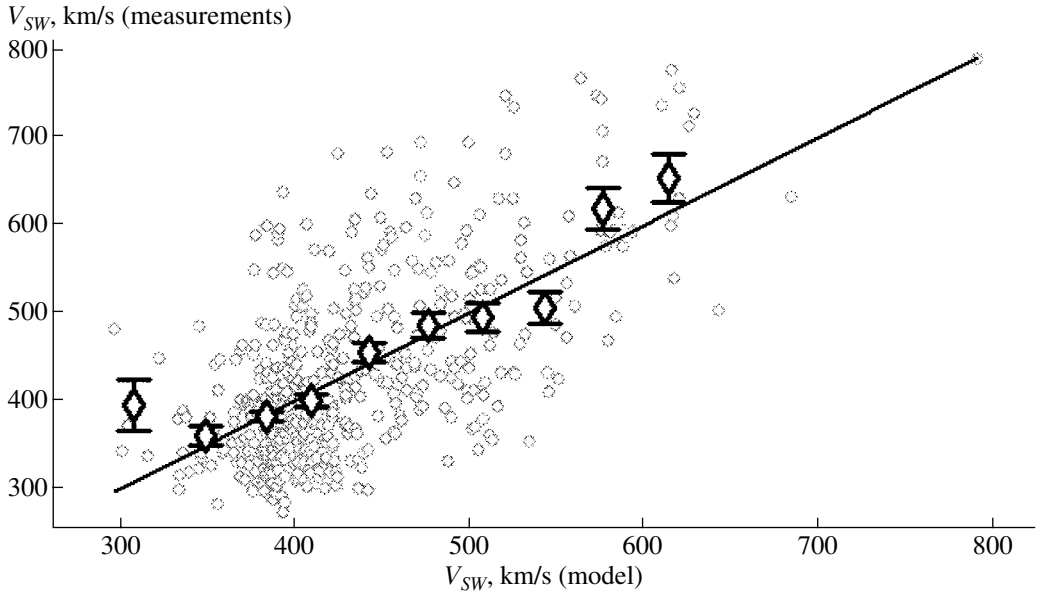

Fig. 1. Correlation between the experimental and calculated daily mean solar-wind velocities. Hereafter, the dots are the data for all days; the diamonds are the result of averaging over equal variation intervals of the abscissa (the mean values are given with a standard statistical error); the straight line corresponds to the linear regression.

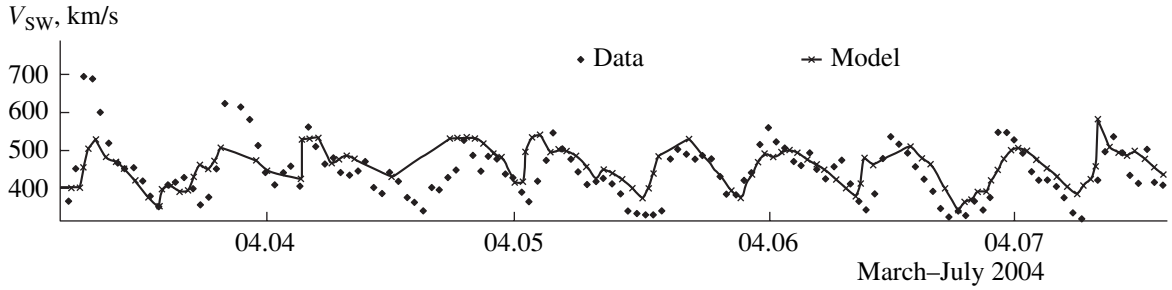

Fig. 2. Behavior of the actually observed and calculated daily mean solar-wind velocities in 2004.

cess, the weak fields can be replaced by stronger ones, which do not always conserve the initial polarity.

To take this into account, we have introduced the polarity index p_s of the source-surface magnetic field, which is determined as follows: $p_s = 1$ or -1 if $B_s > B_u$ or $B_s < -B_u$, respectively. For the other, intermediate values, $p_s = B_s/B_u$. It turned out that the median value of the B_s modulus could be successfully used as a critical value of B_u. For our sample, $B_u = \mathrm{med}|B_s| = 9.08$ μT.

In the absence of interplanetary interactions, the radial field B_s near the Earth must be transformed into the field directed along the helical field line at an angle $\psi = \arctan(\Omega R_E/V_{SW})$ to the radius, where Ω is the solar rotation rate. Let us calculate the IMF projection onto the field line near the Earth expected in accordance with the given V_{SW} value: $B_L = B_{xe}\cos\psi + B_{ye}\sin\psi$, where B_{xe} and B_{ye} are the field components in the ecliptic plane. This projection will be called the IMF longitudinal component. The signs in the latter expression are selected so that positive B_L values would correspond to the direction from the Sun. The linear regression model:

$$B_L(t) = (0.4 \pm 0.1) + (3.4 \pm 0.4)p_s(t-\tau) + (0.04 \pm 0.01)B_s(t-\tau) - (0.0003 \pm 0.0001)B_p(t-\tau) \quad (3)$$

makes it possible to determine the IMF longitudinal component with the correlation coefficient $\rho = 0.79$ and the rms deviation $\sigma = 2.4$ nT (Fig. 5).

As seen from Fig. 6 plotted for several months of 2004, model (3) describes the sector structure and other particularities of the IMF behavior.

Because of gaps in the data, we again (as in the case of the solar wind velocity) had to apply the model based on the strictly selected data for the entire period under discussion (1976–2004) to all data available in a limited

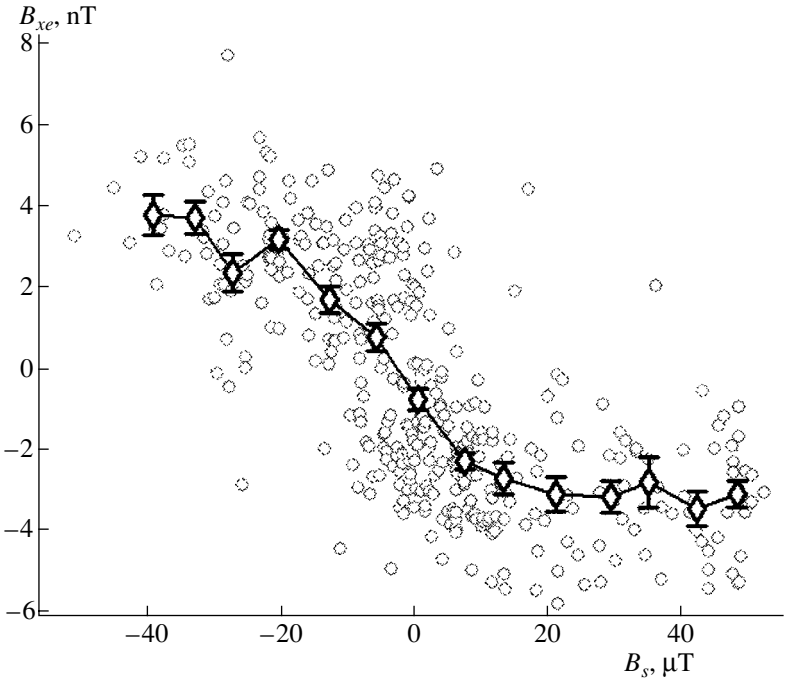

Fig. 3. Relation between the daily mean magnetic field B_s (Earth's projection onto the source surface) and IMF radial component near the Earth.

time interval. However, the model, even deliberately degraded, yields useful results. An additional analysis shows that the discrepancy between the model and experiment is most significant in the periods of interplanetary disturbances associated with sporadic events in the Sun.

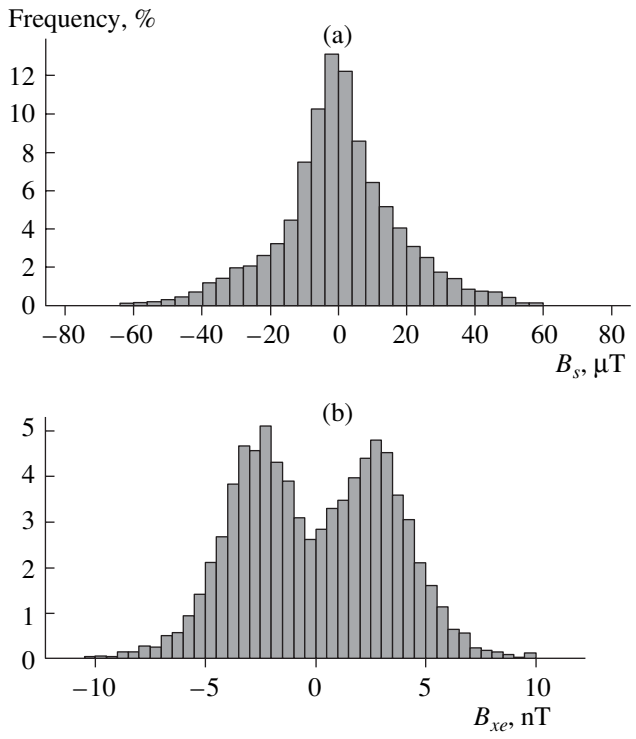

Fig. 4. Distribution of the magnitudes of the daily mean magnetic field B_s and IMF radial component near the Earth (1976–2004).

Using $|B_s|$ (with a small contribution of $|B_p|$), we obtain a model for the intensity of the interplanetary magnetic field B:

$$B(t) = (5.1 \pm 0.1) + (0.043 \pm 0.006)|B_s|(t-\tau) + (0.00010 \pm 0.00007)|B_p|(t-\tau), \quad (4)$$

which agrees with observations with the rms deviation $\sigma = 1.5$ nT.

Model of the IMF B_z component. Depending on the season, one or other part of the IMF ecliptic component is projected onto the axis of the Earth's magnetic dipole. Since the projection of the magnetic dipole axis completes one rotation in the ecliptic plane for a year and the IMF ecliptic component is determined by B_s, the IMF B_z component in the geomagnetic coordinate system (B_{zm}) will depend on $B_s\sin(2\pi t/T)$ and $B_s\cos(2\pi t/T)$, where $T = 1$ year. In fact, the values of B_{zm} determined defined by the model

$$B_{zm}(t) = (-0.09 \pm 0.06) + (0.042 \pm 0.004) \times B_s\sin(2\pi t/T) - (0.014 \pm 0.004)B_s\cos(2\pi t/T), \quad (5)$$

(where the time t is, for definiteness, counted from the winter solstice) correlate with the really measured values ($\rho = 0.48$, $\sigma = 1.10$ nT) (Fig. 7).

Prediction of the *Ap* index of geomagnetic activity. It is clear that the magnetic field B_s obtained at the

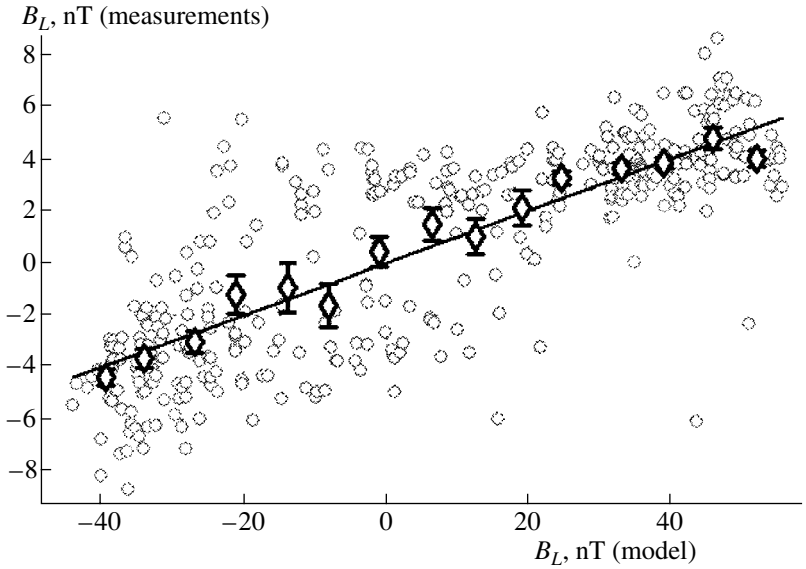

Fig. 5. Correlation between the experimental and calculated daily mean values of the IMF longitudinal component near the Earth.

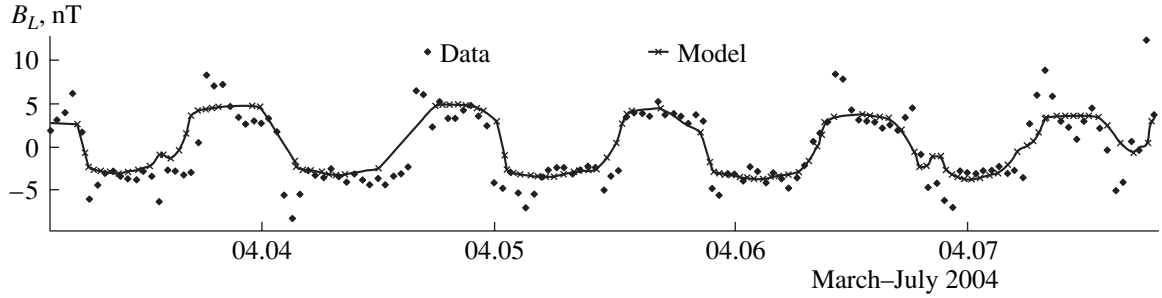

Fig. 6. Behavior of the experimental and calculated daily mean values of the IMF longitudinal component near the Earth during March–July 2004.

source surface can be used to estimate the IMF absolute value and various components and the solar-wind velocity near the Earth, i.e., nearly all basic geoeffective parameters of the solar wind.

To estimate the energy coming into the magnetosphere, Akasofu [1981] proposed the parameter:

$$E_A = V_{SW}B^2L_0^2\sin^4(\theta/2), \quad (6)$$

where L_0 is the radius of the dayside magnetopause, and θ is the IMF inclination angle with respect to the plane of the magnetic equator. The parameter E_A controls the level of geomagnetic activity fairly well. To make sure of this, we calculated E_A for each hour of the days in our sample and obtained the correlation between the daily mean values of E_A and *Ap* indices of geomagnetic activity with a correlation coefficient of 0.77. Equations (2)–(6) allow us to determine the Akasofu parameter E_{AS} directly from the solar magnetic data. Unfortunately, we have not hourly mean solar data, which makes the E_{AS} estimate rough. Nevertheless, the E_{AS} values proved to correlate both with E_A ($\rho = 0.43$) and (somewhat better) with the *Ap* indices ($\rho = 0.46$).

The result will be even better if we combine the parameters determining V_{SW}, B, and B_{zm} in a single linear regression model for *Ap*.

$$\begin{aligned} Ap = {} & (7.1 \pm 0.6) + (22 \pm 3)W_s + (0.15 \pm 0.03)|B_s| \\ & - (0.19 \pm 0.03)B_s\sin(2\pi t/T) \\ & + (0.05 \pm 0.03)B_s\cos(2\pi t/T). \end{aligned} \quad (7)$$

The *Ap* values calculated from this expression correlate with the observed ones with the coefficient $\rho = 0.52$ (Fig. 8).

This must be considered a good correlation. The fact is that Eq. (7) factually predicts the *Ap* index, on the average, for 4 days ahead. A reliable forecast of geomagnetic activity for such a long term is beyond the capabilities of any existing prognostic center. For

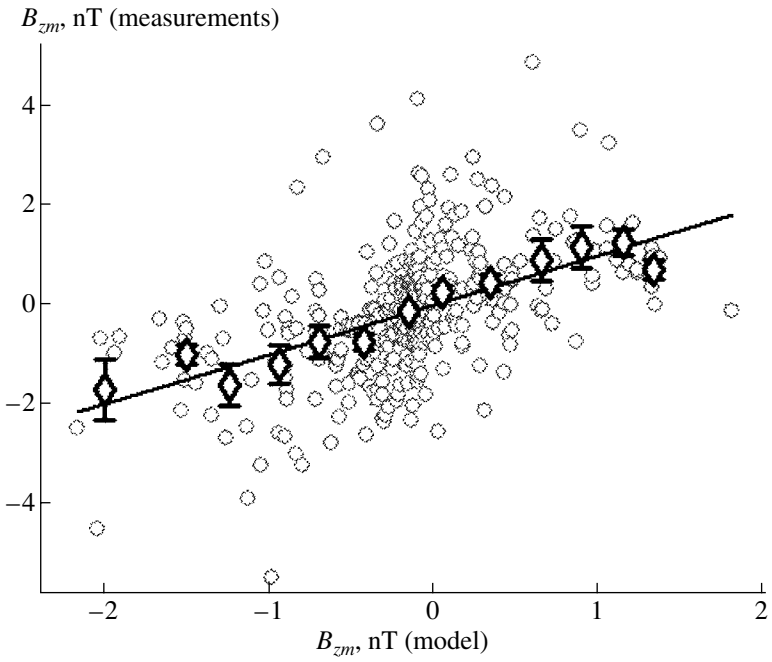

Fig. 7. Correlation between the experimental and calculated daily mean values of the IMF B_z component in the geomagnetic coordinate system.

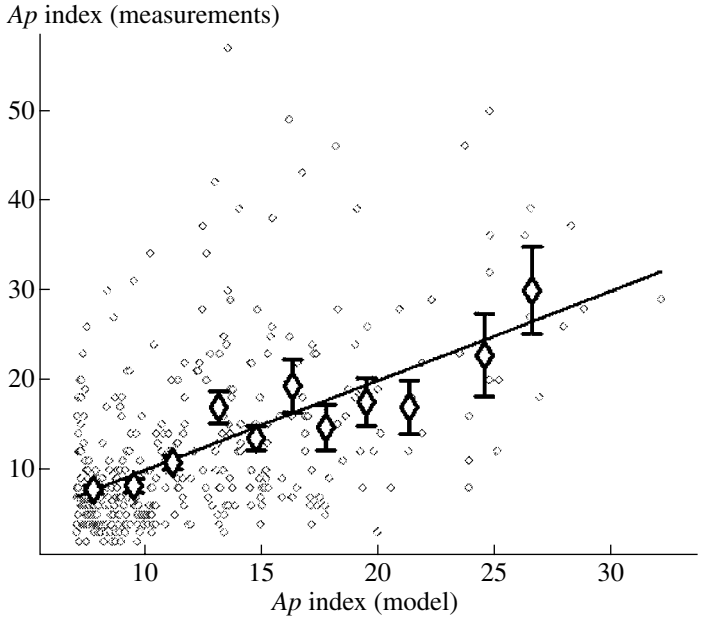

Fig. 8. Correlation between the experimental and calculated daily mean *Ap* indices of geomagnetic activity.

example, the three-day forecasts of the daily mean *Ap* index issued by NOAA/SEC and the Australian Prognostic Agency (IPS) in 1999–2004 were realized with a correlation coefficient of 0.26–0.28 [Oraevsky et al., 2002; Belov et al., 2005]. It means that the available prediction methods give half as good agreement with observations as the model under discussion, whose practical use could, therefore, significantly improve the short-term forecasts.

CONCLUSIONS

The magnetic field parameters calculated for the Earth's projection on the solar-wind source surface can

be used to forecast the solar-wind velocity, the main properties of IMF near the Earth, and the level of geomagnetic activity under quiet and moderately disturbed conditions. This conclusion is inferred from the statistical analysis of a limited number (about 400 points) of specially selected days, but we are sure that it is related to most periods, except for the days when ejections of solar matter reach the Earth or their impact is essential.

The empirical relations revealed here can find practical use and actually improve the short-term geomagnetic forecasts. This only requires reliable measurements of the solar magnetic field and their prompt (daily or more frequent) processing. It would be best to rely on the satellite (weather-independent) magnetic measurements like those carried out within the frames of the SOHO/MDI experiment. We believe that the use of such data is not only the way of introducing the method under discussion into practice but also the best way of updating this method. If we use the measurements for a single day instead of a synoptic magnetic map, the nonstationary solar events will affect the data for the given day but not for the entire rotation. Besides, the field at the center of the disk will be determined more precisely. Alternative opportunities for improving the forecast technique may be associated, for example, with using more sophisticated models and rejecting the linearity condition.

Of course, the forecasting method under discussion should complement rather than substitute the other existing methods. For example, in forecasting the geomagnetic activity, this method can be readily combined with the traditional technique taking into account the inertia, 27-day recurrence, and seasonal variation. Such a combination will provide a sound background forecast of the *Ap* index for most of the time, which, in turn, must be complemented with a forecast of fast traveling interplanetary disturbances based on observations of the solar sporadic events.

ACKNOWLEDGMENTS

This work was supported by the Russian Foundation for Basic Research, project nos. 04-02-16763, 05-02-16090, and 05-02-17251.

REFERENCES

1. S. I. Akasofu, "The Solar Wind–Magnetosphere Energy Coupling and Magnetosphere Disturbances," Planet. Space Sci. **28**, 495–509 (1980).
2. A. V. Belov, S. P. Gaidash, Kh. D. Kanonidi, et al., *Operative Center of the Geophysical Prognosis* (IZMIRAN, 2005), Ann. Geophysical **23** (9), 3163–3170 (2005).
3. J. T. Hoeksema and P. H. Scherrer, *The Solar Magnetic Field* (Rep. UAG-94, NOAA, Boulder, 1986).
4. V. N. Obridko, B. D. Shelting, and A. F. Kharshiladze, "Multiparametric Calculations of the Solar Wind Parameters from Data on the Solar Magnetic Field," Astron. Vestn. **38** (3), 261–272 (2004).
5. V. N. Obridko, B. D. Shelting, and A. F. Kharshiladze, "Near-Earth Magnetic Field Calculations from Data on Solar Magnetic Field," Geomagn. Aeron. **46** (3), 2006.
6. V. N. Obridko, A. F. Kharshiladze, and B. D. Shelting, "On calculating the solar wind parameters from the solar magnetic field data," Astron. Astrophys. Trans. **11**, 65–79 (1996)
7. V. N. Oraevsky, Kh. D. Kanonidi, A. V. Belov, and S. P. Gaidash, "Operative Center IZMIRAN on Forecasting of Heliophysical Conditions. Problem of the Forecasting of Extreme Situations and Their Sources," in *Proceedings of the Research–Practical Conference on 26–27 June 2001* (Center "Antistikhiya", 2002), pp. 222–229.
8. Y. M. Wang and N. R. Sheeley, "On Potential Field Models of the Solar Corona," Astrophys. J. **392**, 310–319 (1992).
9. Y. M. Wang and N. R. Sheeley, "Solar Wind Speed and Coronal Flux Tube Expansion," Astrophys. J. **335**, 726–732 (1990).
10. Y. M. Wang and N. R. Sheeley, "Why Fast Solar Wind Originates from Slowly Expanding Coronal Flux Tubes," Astrophys. J. **372**, L45–48 (1991).
11. Y. M. Wang, "Energy Coupling between the Solar Wind and the Magnetosphere," Space Sci. Rev. **28**, 121 (1981).